Research Article

Journal of Innate Immunity

J Innate Immun 2016;8:517–528
DOI: 10.1159/000447713

Received: February 24, 2016
Accepted after revision: June 20, 2016
Published online: July 16, 2016

Induced Disruption of the Iron-Regulatory Hormone Hepcidin Inhibits Acute Inflammatory Hypoferraemia

Andrew E. Armitage[b] Pei Jin Lim[b] Joe N. Frost[b] Sant-Rayn Pasricha[b] Elizabeth J. Soilleux[c] Emma Evans[a] Alireza Morovat[d] Ana Santos[e] Rebeca Diaz[e] Daniel Biggs[e] Benjamin Davies[e] Uzi Gileadi[b] Peter A. Robbins[f] Samira Lakhal-Littleton[f] Hal Drakesmith[b, g]

[a]Department of Biochemistry, Birmingham Heartlands Hospital, Heart of England NHS Foundation Trust, Birmingham, [b]MRC Human Immunology Unit, MRC Weatherall Institute of Molecular Medicine, University of Oxford, [c]Nuffield Division of Clinical Laboratory Sciences, Radcliffe Department of Medicine, University of Oxford and [d]Department of Clinical Biochemistry, Oxford University Hospitals NHS Foundation Trust, [e]Wellcome Trust Centre for Human Genetics and [f]Department of Physiology, Anatomy and Genetics, University of Oxford, and [g]BRC Blood Theme, NIHR Oxford Biomedical Research Centre, Oxford, UK

Key Words
Iron · Inflammation · Hepcidin · Hypoferraemia

Abstract
Withdrawal of iron from serum (hypoferraemia) is a conserved innate immune antimicrobial strategy that can withhold this critical nutrient from invading pathogens, impairing their growth. Hepcidin *(Hamp1)* is the master regulator of iron and its expression is induced by inflammation. Mice lacking *Hamp1* from birth rapidly accumulate iron and are susceptible to infection by blood-dwelling siderophilic bacteria such as *Vibrio vulnificus*. In order to study the innate immune role of hepcidin against a background of normal iron status, we developed a transgenic mouse model of tamoxifen-sensitive conditional *Hamp1* deletion (termed i*Hamp1*-KO mice). These mice attain adulthood with an iron status indistinguishable from littermate controls. *Hamp1* disruption and the consequent decline of serum hepcidin concentrations occurred within hours of a single tamoxifen dose. We found that the TLR ligands LPS and Pam3CSK4 and heat-killed *Brucella abortus* caused an equivalent induction of inflammation in control and i*Hamp1*-KO mice. Pam3CSK4 and *B. abortus* only caused a drop in serum iron in control mice, while hypoferraemia due to LPS was evident but substantially blunted in i*Hamp1*-KO mice. Our results characterise a powerful new model of rapidly inducible hepcidin disruption, and demonstrate the critical contribution of hepcidin to the hypoferraemia of inflammation.

Introduction

Iron is required for the proliferation of almost all pathogens, and iron availability within the host critically influences the outcome of infection [1–3]. Under normal conditions, serum iron is tightly chaperoned by transferrin and cellular iron is stored within the protective protein shell of ferritin. In response to infection, iron avail-

KARGER

E-Mail karger@karger.com
www.karger.com/jin

Dr. Hal Drakesmith
MRC Human Immunology Unit, MRC Weatherall Institute of Molecular Medicine
University of Oxford, John Radcliffe Hospital
Oxford OX3 9DS (UK)
E-Mail alexander.drakesmith@imm.ox.ac.uk

ability is further restricted. Notably, serum iron levels can plummet, causing 'the hypoferraemia of infection' [4], and this provides a defence against siderophilic blood-dwelling organisms such as *Vibrio vulnificus* [5].

Ferroportin is the iron export protein that releases iron into serum from enterocytes, red pulp macrophages, Kupffer cells and some hepatocytes [6–8]. The iron regulatory hormone hepcidin inhibits ferroportin [9, 10], and is upregulated by inflammation. Hepcidin's critical role in governing iron homeostasis is demonstrated by hepcidin knockout (*Hamp1*-KO) mice that rapidly and massively accumulate iron from early in life. In addition, *Hamp1*-KO mice have serum iron elevated to such a degree that the binding capacity of transferrin is saturated, leading to the presence of non-transferrin-bound iron [11]. However, this profound effect compromises the utility of *Hamp1*-KO mice for investigating the role of hepcidin under normal iron conditions [12]. Maintaining *Hamp1*-KO mice on iron-deficient diets can equalise serum iron parameters between *Hamp1*-KO and wild-type mice [5]; however, total iron levels and the ratio of serum iron to stored iron within *Hamp1*-KO mice still differ, which is important when investigating alterations in iron trafficking as a result of inflammation.

To address these issues, we developed a novel transgenic mouse in which floxed *Hamp1* alleles can be excised conditionally by activation of a ubiquitously expressed Cre-recombinase that is fused to a mutated oestrogen receptor ligand-binding domain ($CreER^{T2}$). Inducible *Hamp1*-KO mice (that we termed 'i*Hamp1*-KO') grow to adulthood with normal iron stores and serum iron parameters but, upon exposure to tamoxifen, delete *Hamp1* irreversibly. Here we first validate this novel model by investigating the effects of induced hepcidin deletion on long- and short-term iron traffic, and then test the role of hepcidin in acute inflammatory hypoferraemia caused by the administration of LPS, Pam3CSK4 and heat-killed *Brucella abortus* (HKBA).

Materials and Methods

Mice

All animal procedures were performed in a licensed establishment under the authority of the UK Home Office project (PPL40/3636) and personal licenses in accordance with the Animals (Scientific Procedures) Act 1986, and were approved by the University of Oxford ethical review committee.

Mice were bred and housed in individually ventilated cages within the Department of Biomedical Services (University of Oxford). Mice were fed ad libitum with a standard diet containing 188 ppm iron (SDS Dietex Services, diet 801161). C57BL/6 mice were purchased from Harlan Laboratories. To develop an i*Hamp1*-KO model, we used floxed-hepcidin mice on a C57BL/6 background *(Hamp fl/fl)* generated by gene targeting in JM8F6 embryonic stem cells as described *($Hamp^{tm1Wthg}$)* [13]; in these mice, exons 2 and 3 of the *Hamp1* gene are flanked by LoxP sites. These were crossed with B6.129-*$Gt(ROSA)^{26Sortm1(cre/ERT2)Tyj/J}$* mice (referred to henceforth as *$Rosa\text{-}CreER^{T2}$*), which express Cre fused to a modified oestrogen receptor (allowing nuclear translocation, and thus activation, in the presence of tamoxifen) under the control of the ubiquitous *Gt(ROSA)26Sor* promoter [14]. A breeding colony of mice homozygous for the floxed-*Hamp* allele and either heterozygous or wild-type for *$Rosa\text{-}CreER^{T2}$* were generated and crossed to yield 50% Cre-positive *Hamp fl/fl* (termed 'i*Hamp1*-KO' mice) and 50% Cre-negative *Hamp fl/fl* littermate control (termed 'i*Hamp1*-Ctrl') offspring (see online suppl. fig. 1; for all online suppl. material, see www.karger.com/doi/10.1159/000447713).

Induction of Targeted Disruption of Hamp1

To stimulate targeted disruption of the *Hamp1* gene, mice were given 1 mg of tamoxifen (Sigma, T5648) in 100 µl of 10% ethanol (Sigma)/90% corn oil (Sigma) vehicle intraperitoneally. Depending on the experiment, mice were given between 1 and 5 tamoxifen doses over 1–5 days.

Mouse Treatments

For LPS and Pam3CSK4, mice were given 1 µg/g of *E. coli* LPS-055:B5 (Sigma, L2880) or 400 ng/g Pam3CSK4 (Invivogen) diluted in Dulbecco's PBS (Lonza) intraperitoneally, and were culled after 6 or 3 h, respectively. For HKBA, mice were given 2.5×10^8 HKBA particles (strain 1119-3, grown and heat inactivated at the Animal and Plant Health Agency, Weybridge, UK) in 200 µl of Dulbecco's PBS (Lonza) intraperitoneally, and were culled 6 h later.

Genotyping

Genotyping was performed initially using DNA extracted from ear notches, with subsequent confirmation using DNA extracted from the liver; DNA was extracted using the Isolate II Genomic DNA Kit (Bioline) or by alkaline lysis (25 mM NaOH/0.2 mM EDTA) at 95°C followed by neutralisation (40 mM Tris-HCl; ear notches only). Genotyping PCRs were performed using MyTaq Red mix (Bioline) to detect: (a) floxed or wild-type *Hamp1* alleles, (b) deleted *Hamp1*, and (c) *Cre*. The primers and cycling conditions are described in the online supplementary materials.

Gene Expression Analysis

Liver and spleen explants (approximately 1–2 mm^3) or whole-lung lobes were stored immediately after culling mice in RNAlater (Life Technologies); duodenum was snap-frozen and explants were subsequently used for RNA isolation. RNA was extracted, cDNA prepared and gene expression quantified (using inventoried TaqMan assays; online suppl. table 1) as described [15].

Serum Measurements

Blood was taken by cardiac puncture immediately after sacrificing the mice. Serum was prepared by the centrifugation of clotted blood at >6,000 *g* for 3–5 min in BD Microtainer SST tubes (Beckton Dickinson); serum aliquots were frozen immediately at –80°C. Serum hepcidin concentrations were quantified by competitive ELISA using the Hepcidin-Murine Compete Kit (Intrinsic Lifesciences) according to the manufacturer's protocol, with sera

diluted to either 5 or 2.5%. Serum iron and unsaturated iron binding capacity (UIBC) were quantified using the MULTIGENT Iron Kit on the Abbott Architect c16000 automated analyser (Abbott Laboratories) [16]. When UIBC data were obtained, transferrin saturation (Tsat) was calculated using: Tsat = [(Serum Iron)/(Serum Iron + UIBC)] × 100. UIBC results returned below the assay lower limit of detection (7.3 μmol/l) were inferred as 0 μmol/l. Serum ferritin concentrations were measured using the Ferritin mouse ELISA Kit (ab157713, Abcam).

Histology: Perls' Staining

Immediately after the mice were culled, tissues (liver, spleen, heart, pancreas) were fixed in 10% neutral-buffered formalin and processed to paraffin. Four-micron sections were stained with Perls' stain using standard techniques. Sections were examined by a specialist haematopathologist and photographed using a Nikon DS-FI1 camera with a Nikon DS-L2 control unit (Nikon UK Ltd) and Olympus BX40 microscope (Olympus UK Ltd).

Tissue Non-Heme Iron Measurement

Tissue samples were dried for 4–6 h at 100°C before weighing. Dried tissue was digested with 10% trichloroacetic acid/30% hydrochloric acid for 20 h at 65°C. Non-heme iron content was measured colorimetrically (OD_{535} nm) against a standard curve generated from ferric ammonium citrate (F5879, Sigma) serial dilutions following reaction with chromogen reagent containing 0.1% (w/v) batho-phenoldisulphonic acid (BPS, 146617, Sigma)/0.8% thioglycolic acid (88652, Sigma).

Statistics

Statistical analyses were performed using Prism 6 (GraphPad software). In cases where data values were spread over orders of magnitude, statistical tests were performed on log-transformed data, and geometric means were plotted on graphs.

Results

Tamoxifen-Induced Hepcidin Disruption in Multiple Tissues and Severe Iron Overload in iHamp1-KO Mice

In order to generate a model in which the gene encoding hepcidin *(Hamp1)* could be selectively, ubiquitously and rapidly disrupted in adult mice, we crossed floxed-hepcidin [13] *(Hamp1^{tm1}fl/fl)* with *Rosa-CreER^{T2}* mice (online suppl. fig. 1). We termed the resultant mouse, homozygous for the floxed-*Hamp1* gene and heterozygous for *Rosa-CreER^{T2}*, the 'i*Hamp1*-KO' mouse, and Cre-negative littermate controls 'i*Hamp1*-Ctrl' mice. Tamoxifen administration to i*Hamp1*-KO mice permits nuclear access for the CreER^{T2} protein that consequently mediates the excision of exons 2–3 of the *Hamp1* gene, resulting in a null allele. The loss of hepcidin activity would be expected to lead to iron accumulation over time.

We first treated 7-week-old male i*Hamp1*-Ctrl and i*Hamp1*-KO mice (fig. 1a) with tamoxifen daily for 5 consecutive days and analysed mice 3 months later. The deleted *Hamp1* allele (481 bp) was detected in the ear, liver, duodenum and spleen (fig. 1b). Deletion of exons 2 and 3 was associated with a marked loss of *Hamp1* mRNA detection in the liver, spleen, lung and duodenum (fig. 1c) and significant loss of serum hepcidin (fig. 1d).

Tamoxifen-induced i*Hamp1*-KO mice displayed significant liver iron loading, preferentially around perivenular areas (fig. 2a, b). Iron loading was also evident in cardiomyocytes in the heart and in pancreatic parenchyma (online suppl. fig. 2A, B). Conversely, induced i*Hamp1*-KO mice showed no stainable iron in the spleen (fig. 2c, d), consistent with the uninhibited release of iron from red pulp macrophages. Hepatic expression of *Bmp6* mRNA (increased by iron loading [17]) was significantly elevated in induced i*Hamp1*-KO mice (fig. 2e). Serum iron was significantly elevated, such that transferrin was fully saturated (fig. 2f, g), and serum ferritin was consistently raised with increased tissue iron storage (fig. 2h).

Together, these data demonstrate that the *Hamp1* gene can be disrupted in adult i*Hamp1*-KO mice through tamoxifen administration, resulting in the loss of hepcidin expression and induction of an iron-overloading phenotype over 3 months.

Non-Induced iHamp1-KO Mice Have Equivalent Iron Status to Littermate Controls

Our intention was to use *iHamp1*-KO mice for investigating the role of hepcidin against a background of normal iron status. In order to satisfy this criterion, we compared the iron status of non-induced i*Hamp1*-KO mice to that of i*Hamp1*-Ctrl mice. The deleted *Hamp1* allele was not detected in either non-tamoxifen-treated 6-month-old male i*Hamp1*-Ctrl or i*Hamp1*-KO mice (online suppl. fig. 3A; compare with fig. 1a) consistent with no detectable Cre leakage and retention of intact *Hamp1* alleles in non-induced mice. Accordingly, there were no significant differences in liver *Hamp1* mRNA expression, serum hepcidin or serum iron concentrations, or liver *Bmp6* mRNA between groups (online suppl. fig. 3B–E). There was no evidence of liver iron loading by Perls' staining in either i*Hamp1*-Ctrl or i*Hamp1*-KO mice (online suppl. fig. 3F), and both groups displayed stainable macrophage iron in the spleen (online suppl. fig. 3G). Therefore, the hepcidin and iron status of non-induced i*Hamp1*-KO mice at 6 months is equivalent to that of littermate controls.

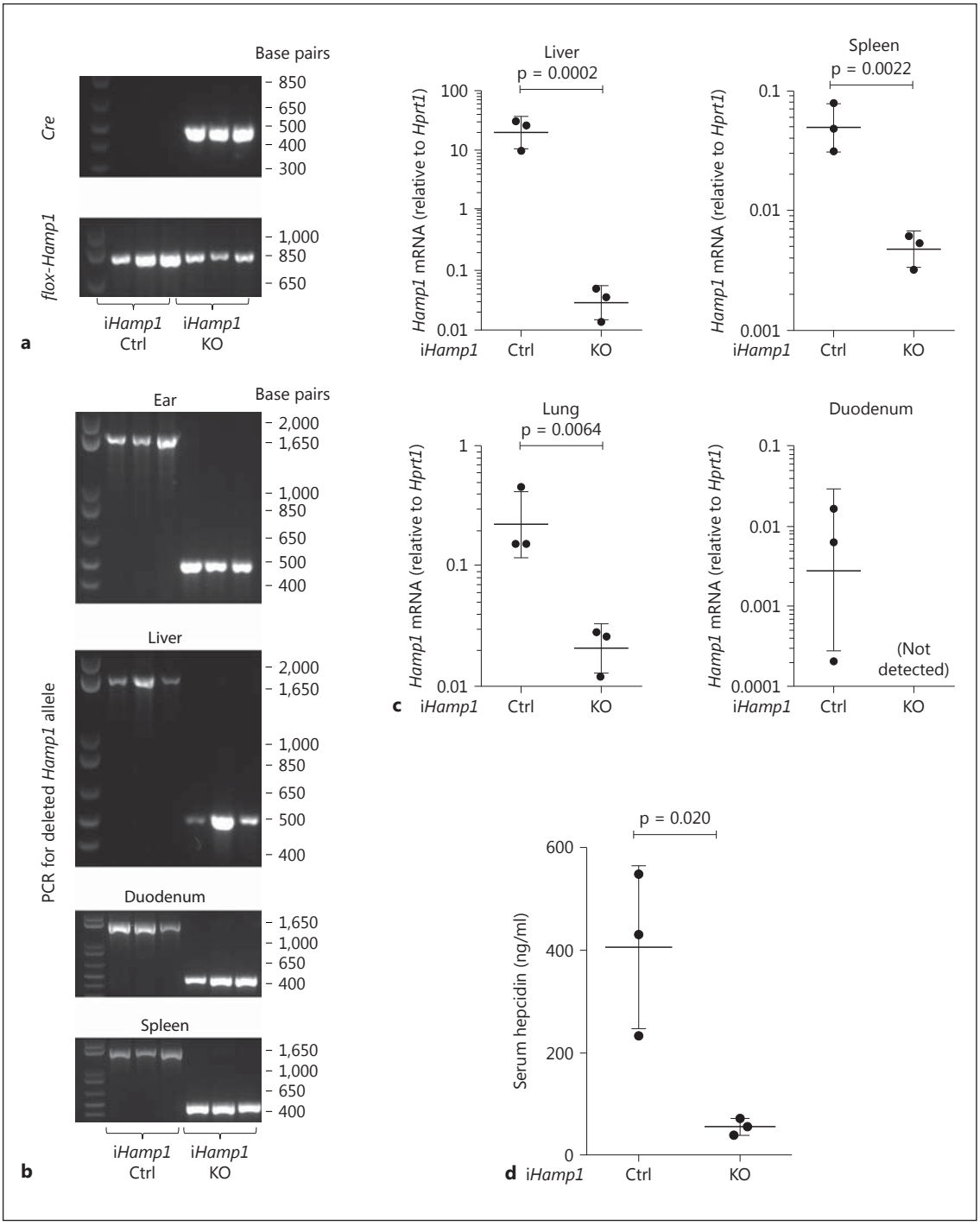

Fig. 1. Induction of targeted disruption of *Hamp1* following tamoxifen administration to i*Hamp1*-KO mice. Seven-week-old male i*Hamp1*-KO mice and littermate i*Hamp1*-Ctrl mice were treated daily for 5 days with 1 mg of tamoxifen per mouse; 3 months later, the mice were sacrificed and tissues taken for analysis. **a** Genotyping PCR from ear tissue confirming the presence of the *Cre* allele (upper panel) in i*Hamp1*-KO but not *iHamp1*-Ctrl mice (lower panel) despite the presence of the *flox-Hamp1* allele in both (761 bp). **b** Genotyping PCR confirming deletion of *Hamp1* exons 2–3 in the ear, liver, duodenum and spleen in tamoxifen-induced i*Hamp1*-KO mice, but not i*Hamp1*-Ctrl mice. **c** Significant depletion of *Hamp1* mRNA in the liver, lung, spleen and duodenum in tamoxifen-induced i*Hamp1*-KO mice compared to i*Hamp1*-Ctrl mice, quantified by qRT-PCR (dot plots show the geometric mean ± geometric SD, with p values reflecting the results of t tests based on log-transformed data). **d** Significant decrease in serum hepcidin in tamoxifen-induced i*Hamp1*-KO mice. Dot plot shows the arithmetic mean ± SD; t test.

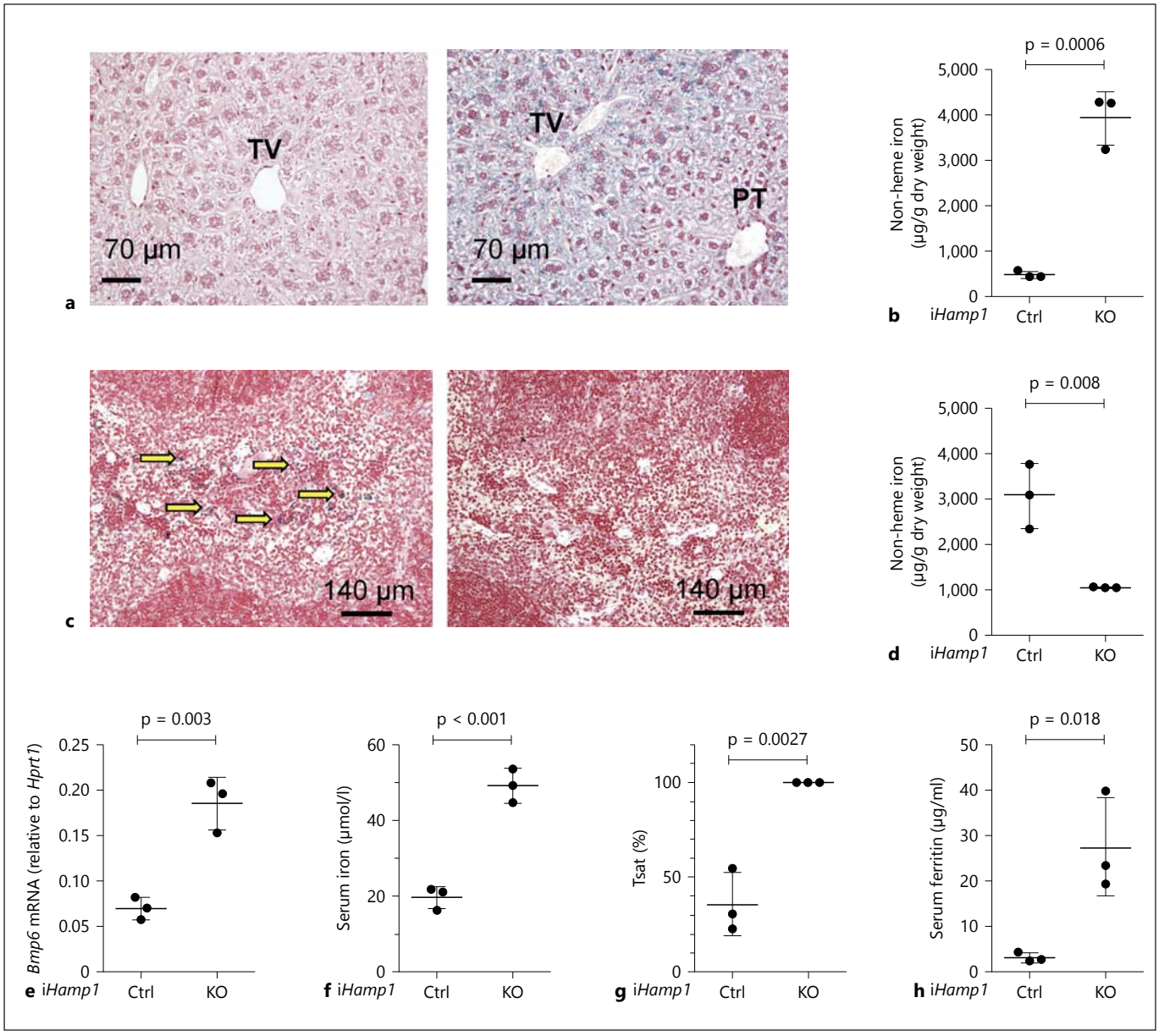

Fig. 2. Evidence of iron loading 3 months after tamoxifen-administration to i*Hamp1*-KO mice. Seven-week-old male i*Hamp1*-KO mice and littermate i*Hamp1*-Ctrl mice were treated daily for 5 days with 1 mg of tamoxifen per mouse; 3 months later, the mice were sacrificed and tissues taken for analysis. Comparisons between tamoxifen-induced i*Hamp1*-KO and littermate *iHamp1*-Ctrl mice. **a** Perls' staining of 4-µm liver sections indicating no iron loading around the terminal venule (TV) in i*Hamp1*-Ctrl mice (left), but increasing iron loading towards the TV compared to the portal triad (PT) in induced i*Hamp1*-KO mice (right). **b** Non-heme liver iron quantification. **c** Perls' staining of 4-µm spleen sections with macrophage iron staining in i*Hamp1*-Ctrl spleens (left) indicated with yellow arrows, absent in induced i*Hamp1*-KO mice. **d** Non-heme spleen iron quantification. **e** Elevated *Bmp6* mRNA. **f** Serum iron. **g** Tsat (the dataset includes imputed Tsat values: when UIBC was below limit of detection, Tsat was allocated the value of 100%) **h** Serum ferritin in *iHamp1*-KO mice. Images were obtained using a Nikon DS-FI1 camera with a Nikon DS-L2 control unit and an Olympus BX40 microscope. Dot plots show the arithmetic mean ± SD; p values indicate the results of t tests. For colors, see online version.

*Short-Term Effects of Tamoxifen Administration in i*Hamp1*-KO and Control Mice*

We next tested the effects of varying the schedule of tamoxifen administration on hepcidin deletion and iron phenotype in i*Hamp1*-KO mice in the short term. Increasing the number of daily tamoxifen doses administered to i*Hamp1*-KO mice cumulatively reduced liver *Hamp1* mRNA and serum hepcidin at 3 days after the final tamoxifen injection (fig. 3a, b). However, a single tamoxifen dose was still able to deplete both parameters, and was also sufficient to significantly increase serum iron and Tsat (fig. 3c, d). To investigate how rapidly hepcidin disruption occurred, we reduced the time between a single tamoxifen dose and analysis. The deleted *Hamp1* allele could be detected in the liver as early as 6 h after tamoxifen administration (fig. 3e; online suppl. fig. 4A), with corresponding significant reductions in serum hepcidin and liver *Hamp1* mRNA (fig. 3f, g; online suppl. fig. 4B, C) and elevations in serum iron (fig. 3h; online suppl. fig. 4D, E) observed by 24 h post-tamoxifen; indeed, only 6 h after tamoxifen, these parameters were significantly altered in female mice (online suppl. fig. 4). The higher hepcidin levels in male (fig. 3e, f) and female (online suppl. fig. 4B, C) i*Hamp1*-Ctrl mice at the 6-hour time point, compared to the 24- and 72-hour time points, likely relate to the time of day that experiments were terminated: 6-hour samples were taken in the afternoon when hepcidin levels are raised, while 24- and 72-hour samples were taken in the morning. To summarise, in adult mice, changes in serum iron levels following *Hamp1* disruption occur rapidly, reflecting the sensitive control of serum iron by hepcidin.

To ensure that these effects were not related to tamoxifen itself, we examined changes in hepcidin and serum iron in tamoxifen-treated wild-type C57BL/6 mice and i*Hamp1*-Ctrl mice. Liver *Hamp1* mRNA levels were equivalent in vehicle- and tamoxifen-treated C57BL/6 mice 6 h after a single tamoxifen dose, but were marginally lower in tamoxifen-treated wild-type mice by 24 h, possibly due to the structural similarity between tamoxifen and oestrogen, which can suppress hepcidin [18] (online suppl. fig. 5A). At the same time point, there was a slight but significant decrease (as opposed to expected increase) in serum iron, but no difference in Tsat (online suppl. fig. 5B, C).

At 30 h post-tamoxifen administration – the afternoon time point equivalent to that used in the following experiments assessing the effect of hepcidin disruption on inflammatory hypoferraemia – tamoxifen-treated male and female C57BL/6 mice had equivalent liver *Hamp1* mRNA expression to vehicle-treated controls, although baseline Hamp1 expression was higher in females (online suppl. fig. 6A) as previously reported [19]. A modest decrease in serum hepcidin was observed in female mice (online suppl. fig. 6B), which again may relate to oestrogen-related hepcidin suppressive effects. However, this did not manifest as confounding changes in serum iron (online suppl. fig. 6C), and was not associated with alterations *Id1* mRNA, reflecting perturbation of the hepcidin-stimulatory BMP (bone morphogenetic protein) pathway, nor Stat3-signalling as indicated by fibrinogen alpha chain *(Fga*; online suppl. fig. 6D, E).

In i*Hamp1*-Ctrl mice, we found no difference in liver *Hamp1* mRNA or serum iron levels between vehicle- and tamoxifen-treated groups at 3 days post-tamoxifen administration (online suppl. fig. 5A, B). These data show that tamoxifen had at most mild hepcidin-suppressive effects but that these were not accompanied by increases in serum iron. Although there are sex-dependent effects on baseline iron status (as previously observed), the *Hamp1* allele is disrupted in both male and female mice in response to tamoxifen, with rapid and marked effects on serum iron. The results in i*Hamp1*-KO mice are therefore unlikely to be significantly affected by the tamoxifen administration.

Hepcidin Is Required for Maximal Induction of Hypoferraemia in Response to TLR Agonists and HKBA

We next wished to investigate the role of hepcidin in the hypoferraemic response to inflammation. As inducers of inflammation we first chose the TLR4 ligand LPS and the TLR2 ligand Pam3CSK4, both of which have previously been shown to decrease serum iron in mice [12, 20]. We administered male i*Hamp1*-KO and i*Hamp1*-Ctrl adult mice with 1 dose of tamoxifen and then injected mice with either LPS or vehicle 24 h later, and in a separate experiment with either Pam3CSK4 or vehicle.

Six hours after LPS treatment, liver expression of interleukin-6 *(Il6)*, and the acute phase response gene *Fga* were upregulated (fig. 4a, b), indicating an intact inflammatory response in i*Hamp1*-KO and i*Hamp1*-Ctrl mice. Likewise, splenic expression of splenic ferroportin-1 *(Slc40a1)*, encoding ferroportin, was suppressed in both groups of LPS-treated mice (fig. 4c). In PBS-treated i*Hamp1*-KO mice, tamoxifen reduced liver *Hamp1* mRNA (fig. 4d) and serum hepcidin levels (fig. 4e), and increased serum iron compared to tamoxifen-treated i*Hamp1*-Ctrl mice (fig. 4f). In i*Hamp1*-Ctrl mice, LPS caused a significant upregulation of liver *Hamp1* mRNA (fig. 4d), increase in

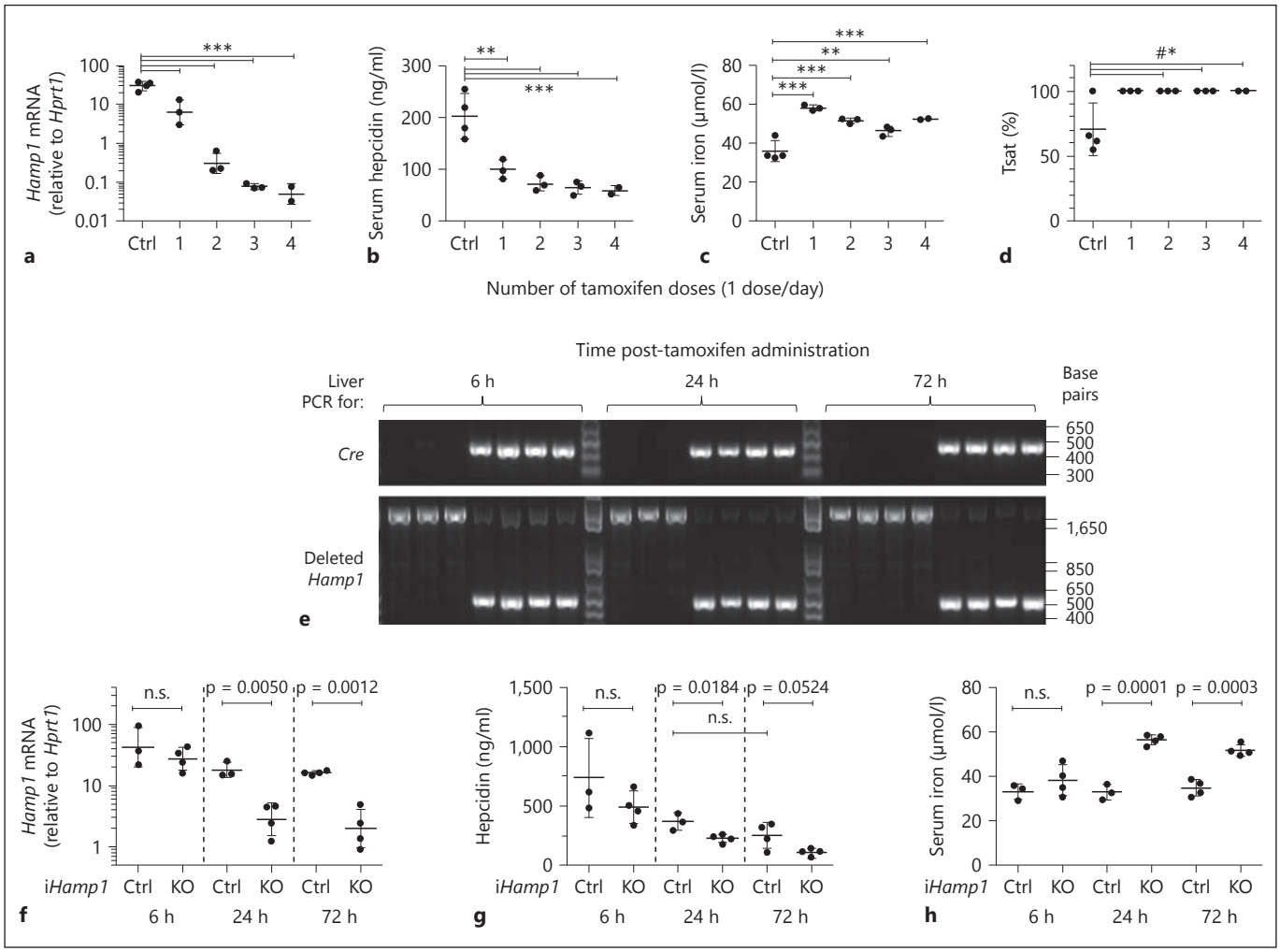

Fig. 3. Effect of the tamoxifen dose and schedule on *Hamp1* disruption in i*Hamp1*-KO mice. **a–d** Seven- to eight-week-old male i*Hamp1*-KO mice were treated with 1 dose of 1 mg of tamoxifen per day, daily for between 1 and 4 days (i.e. 1 dose per day for up to 4 days); littermate i*Hamp1*-Ctrl mice were given 1 tamoxifen dose each day for 4 consecutive days. The mice were sacrificed and tissues taken for analysis 3 days after the last tamoxifen dose. Changes in liver *Hamp1* mRNA ($p < 0.0001$; **a**), serum hepcidin ($p = 0.0002$; **b**), serum iron ($p < 0.0001$; **c**), and Tsat ($p = 0.015$; **d**) with increasing numbers of tamoxifen doses. Dot plots show the arithmetic mean ± SD (except **a**, which shows the geometric mean ± geometric SD, with statistics based on log-transformed data); p values represent the results of one-way ANOVA, with Dunnett's multiple comparison test (*** $p < 0.001$, ** $p < 0.01$, * $p < 0.05$; # dataset includes imputed Tsat values: when UIBC was below the limit of detection, Tsat was allocated the value of 100%). **e–h** Seven- to ten-week-old male i*Hamp1*-KO mice and littermate i*Hamp1*-Ctrl mice were administered a single 1 mg/mouse tamoxifen dose; mice were sacrificed and tissues taken for analysis after 6, 24 or 72 h. **e** PCR detection of *Hamp1* deletion in tamoxifen-induced i*Hamp1*-KO mice, indicated by the presence of a *Cre* allele. **f** Reduction in liver *Hamp1* mRNA in i*Hamp1*-KO mice as early as 6 h post-tamoxifen administration. Changes in serum hepcidin (**g**), and serum iron (**h**). Dot plots show the mean ± SD (except **e**, which shows the geometric mean ± geometric SD, with statistics based on log-transformed data); p values indicate the results of t tests.

serum hepcidin (fig. 4e) and decrease in serum iron (fig. 4f). In induced i*Hamp1*-KO mice LPS did not increase liver *Hamp1* mRNA or hepcidin peptide (fig. 4d, e). LPS was associated with a decrease in serum iron in i*Hamp1*-KO mice suggesting a partial hepcidin-independent contribution to LPS-mediated hypoferraemia, yet serum iron levels still remained significantly higher than in non-LPS-treated i*Hamp1*-Ctrl mice (fig. 4f).

For Pam3CSK4 treatment, we followed the same protocol as for LPS but analysed mice 3 h after administra-

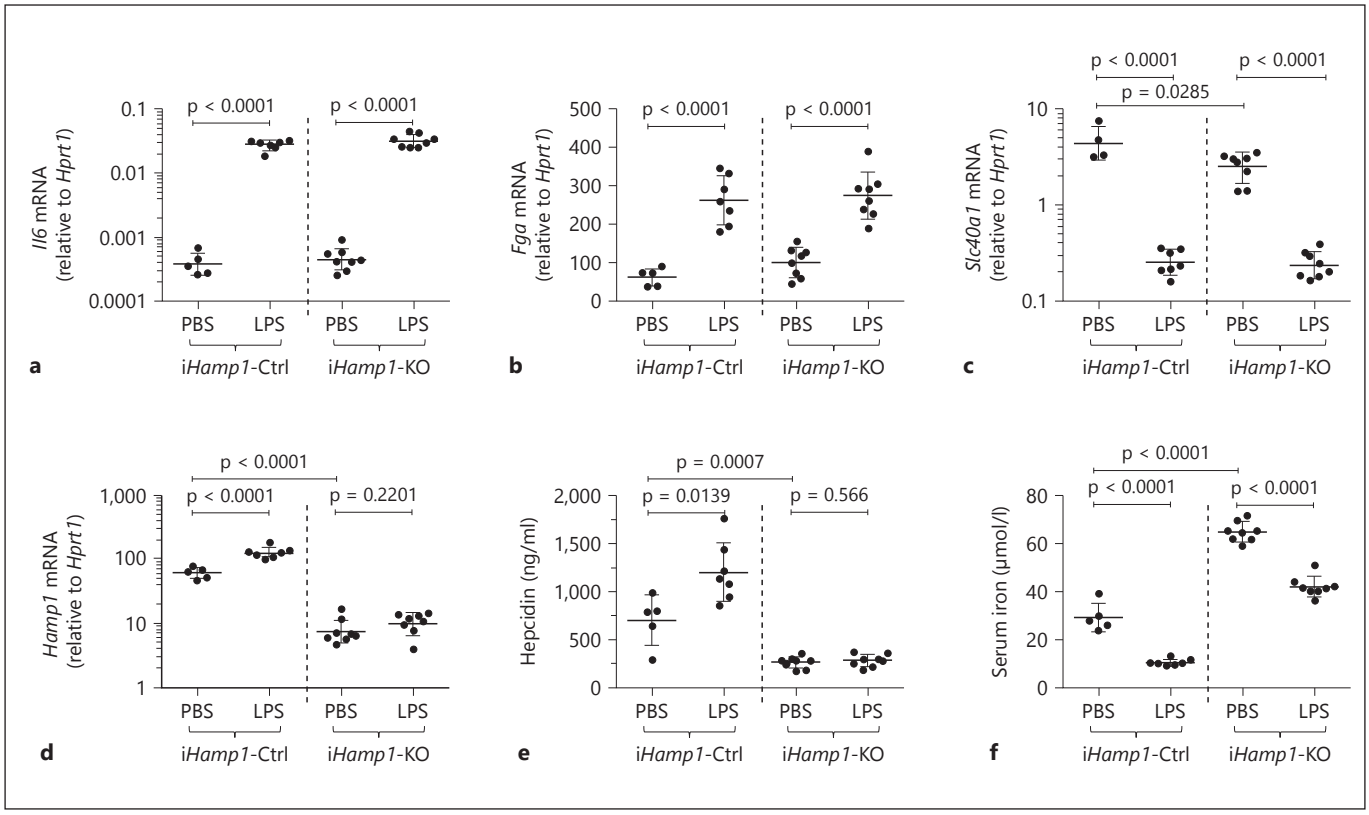

Fig. 4. Effect of tamoxifen-induced hepcidin disruption on the response to LPS in i*Hamp1*-KO mice. Seven- to ten-week-old male i*Hamp1*-KO mice and littermate i*Hamp1*-Ctrl mice were administered 1 mg of tamoxifen per mouse 24 h prior to being given 1 µg/g of LPS (*E. coli* O55:B5) or PBS vehicle intraperitoneally; mice were culled 6 h after LPS administration. Induction of liver *Il6* (**a**) and *Fga* (**b**) mRNA, and reduction of *Slc40a1* mRNA (**c**) in both tamoxifen-treated i*Hamp1*-Ctrl and i*Hamp1*-KO mice treated with LPS. Lack of *Hamp1* mRNA (**d**) and serum hepcidin (**e**) response to LPS in tamoxifen-treated i*Hamp1*-KO mice in contrast to tamoxifen-treated i*Hamp1*-Ctrl mice. **f** Lack of absolute hypoferraemic response to LPS in tamoxifen-treated i*Hamp1*-KO mice. Dot plots show the mean ± SD; p values indicate the results of t tests; in cases where data are spread over orders of magnitude, data are plotted with log scales, geometric means ± geometric SD are shown, and t tests are performed on log-transformed data.

tion of the TLR ligand in line with protocols previously used by others [20]. The results overall were similar to those obtained with LPS in that liver *Il6* and *Fga* were upregulated (fig. 5a, b), and splenic *Slc40a1* was downregulated (fig. 5c) by Pam3CSK4 in both tamoxifen-treated i*Hamp1*-KO and i*Hamp1*-Ctrl mice. However, while Pam3CSK4 increased liver *Hamp1* mRNA and serum hepcidin, and caused a significant drop in serum iron in i*Hamp1*-Ctrl mice, these changes did not occur in i*Hamp1*-KO mice (fig. 5d–f).

We next wished to test the effect of exposing i*Hamp1*-KO mice to intact microbes, and chose HKBA as this treatment has been shown to cause inflammation and hepcidin upregulation [21]. Six hours after HKBA treatment, we observed increased liver *Il6* and *Fga* (fig. 6a, b), and decreased splenic *Slc40a1* (fig. 6c), in both tamoxifen-treated female i*Hamp1*-KO and i*Hamp1*-Ctrl mice. Significant increases in liver *Hamp1* mRNA and serum hepcidin peptide, and a decrease in serum iron, were restricted to HKBA-treated i*Hamp1*-Ctrl mice (fig. 6d–f). Similar patterns of inflammatory responses and hepcidin responses to HKBA we seen in male i*Hamp1*-KO and i*Hamp1*-Ctrl mice (online suppl. fig. 8A–E); in this experiment, although there was no reduction in serum iron in HKBA-treated i*Hamp1*-KO mice, the reduction in serum iron in HKBA-treated littermate control mice was not significant (online suppl. fig. 8F). These experiments show that, when a decrease of serum iron is observed in response to pro-inflammatory stimuli, hepcidin is a non-redundant contributor to inflammation-induced hypoferraemia.

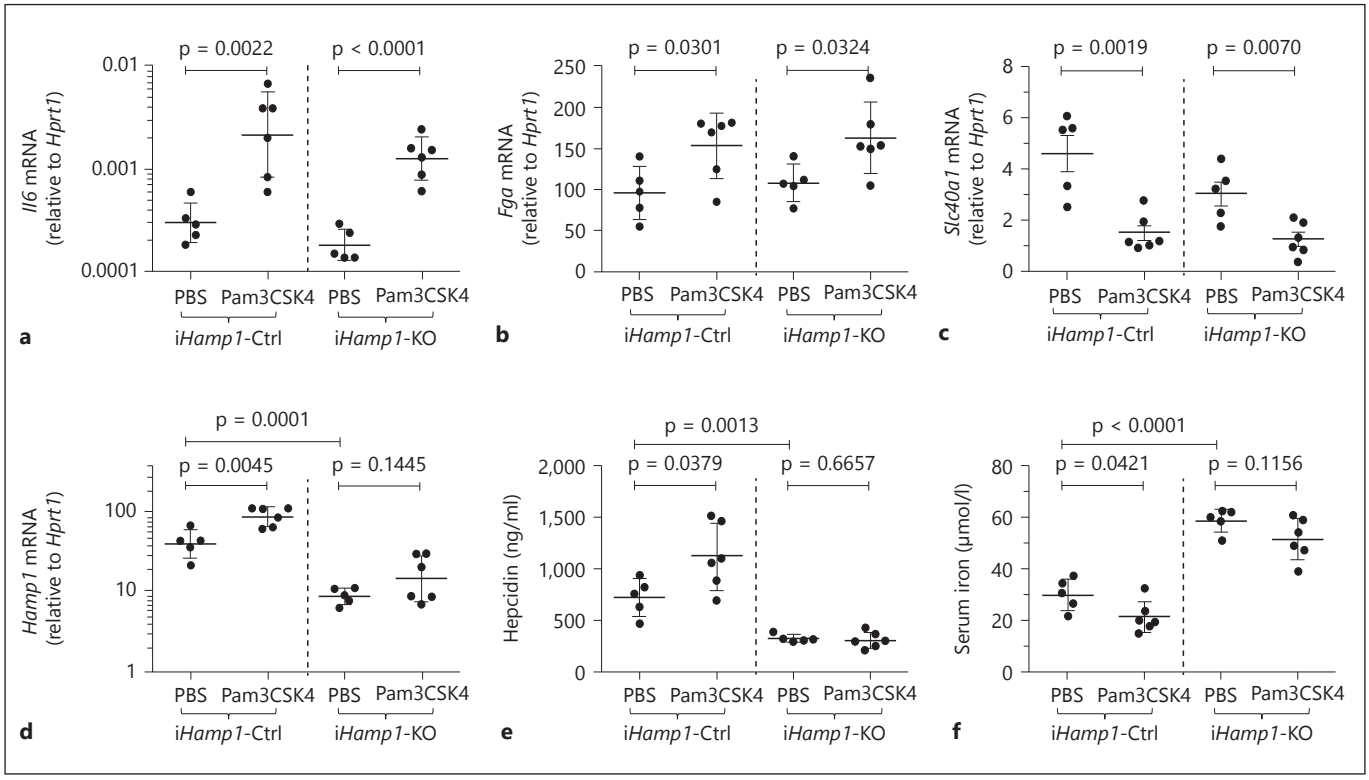

Fig. 5. Lack of hypoferraemic response to the TLR1/2 agonist Pam3CSK4 in tamoxifen-induced i*Hamp1*-KO mice. Eight- to nine-week-old male i*Hamp1*-KO mice and littermate i*Hamp1*-Ctrl mice were administered 1 mg of tamoxifen per mouse 24 h prior to being given 400 ng/g Pam3CSK4 or PBS vehicle intraperitoneally; mice were culled 3 h after LPS administration. Induction of liver *Il6* (**a**) and *Fga* (**b**) mRNA, and reduction of *Slc40a1* mRNA (**c**) in both tamoxifen-treated i*Hamp1*-Ctrl and i*Hamp1*-KO mice treated with Pam3CSK4. Lack of *Hamp1* mRNA (**d**) and serum hepcidin (**e**) response to Pam3CSK4 in tamoxifen-treated i*Hamp1*-KO mice in contrast to tamoxifen-treated i*Hamp1*-Ctrl mice. **f** Lack of hypoferraemic response to Pam3CSK4 in tamoxifen-treated i*Hamp1*-KO mice. Dot plots show the mean ± SD; p values indicate the results of t tests; in cases where data are spread over orders of magnitude, data are plotted with log scales, geometric means ± geometric SD are shown, and t tests are performed on log-transformed data.

Discussion

Hepcidin regulates the rate of iron release from ferroportin-expressing cells, especially macrophages and enterocytes. Hereditary hemochromatosis due to inappropriately low hepcidin concentrations (caused by mutations in *HFE*, *TFR2*, *HJV* or, rarely, *HAMP*) is characterised by increased serum iron and iron accumulation in parenchymal cells, including hepatocytes [reviewed in 22]. Conversely, the injection of hepcidin peptide decreases serum iron [23], and humans or mice with dysfunctional TMPRSS6 have higher hepcidin levels and consequently low serum iron, an impaired capacity to absorb oral iron, and severe iron-restricted erythropoiesis and anaemia [24, 25]. Hepcidin is also increased by inflammation, which may be beneficial in the context of some infections, by withholding iron from the pathogen [5, 26–28].

Current models for studying the physiological role of hepcidin by negating its activity have limitations. Treatments that neutralise circulating hepcidin peptide (anti-hepcidin antibodies and hepcidin-binding L-RNA aptamers) induce a 'rebound' of very high endogenous hepcidin production [29, 30], as the homeostatic machinery attempts to compensate for a lack of active hepcidin. Mice genetically deficient in hepcidin avoid this problem, but rapid iron accumulation from birth means that adult germline *Hamp1*-KO mice have a drastically different iron status compared to wild-type controls [11]. It is therefore difficult to assess the importance of hepcidin upregulation for the inflammatory hypoferraemic response in mice that have such a different baseline iron

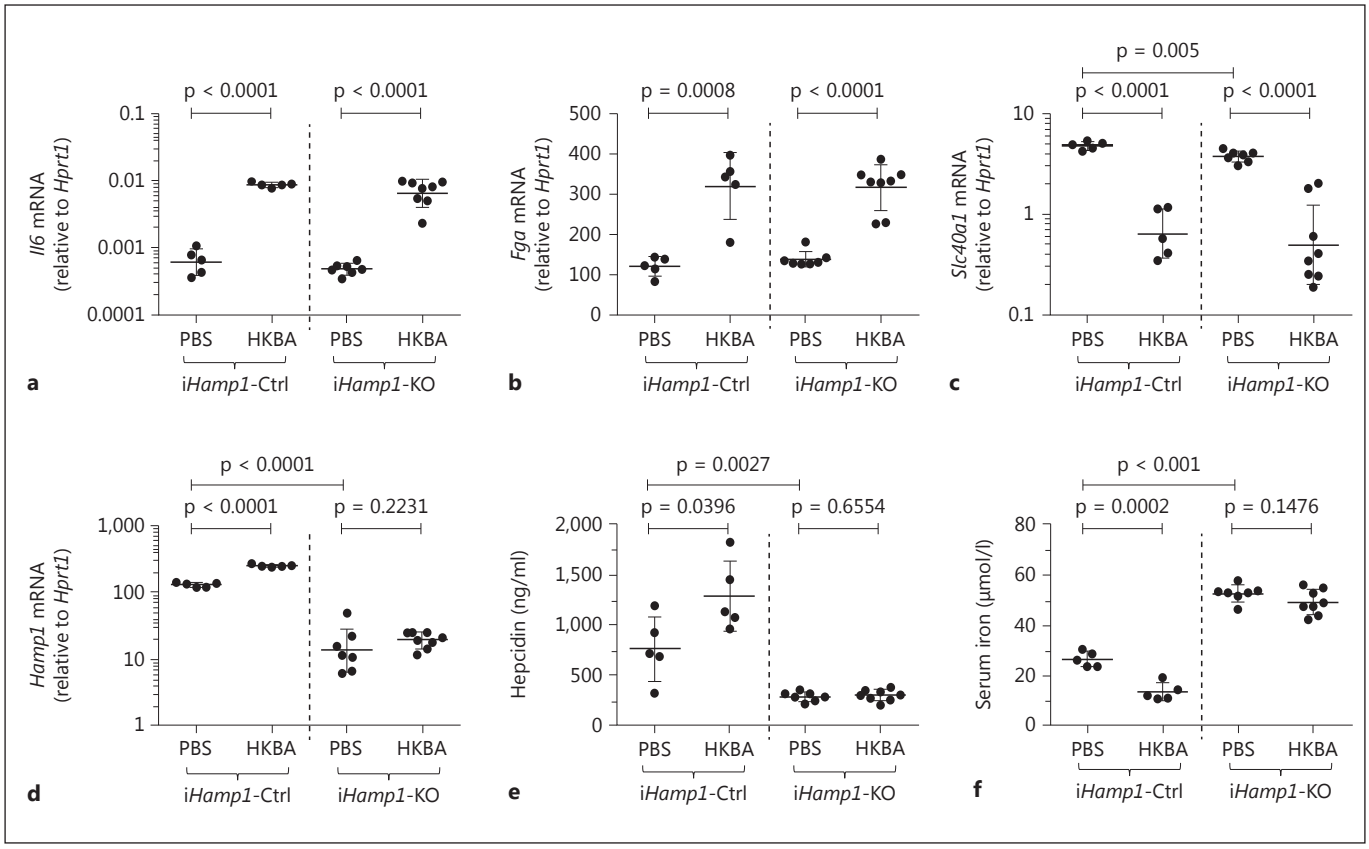

Fig. 6. No hypoferraemic response to HKBA in tamoxifen-induced i*Hamp1*-KO mice. Eight- to nine-week-old female i*Hamp1*-KO mice and littermate i*Hamp1*-Ctrl mice were administered 1 mg of tamoxifen per mouse 24 h prior to being given 2.5×10^8 HKBA or PBS vehicle intraperitoneally; mice were culled 6 h after HKBA administration. Induction of liver *Il6* (**a**) and *Fga* (**b**) mRNA, and reduction of *Slc40a1* mRNA (**c**) in both tamoxifen-treated i*Hamp1*-Ctrl and i*Hamp1*-KO mice treated with HKBA. Lack of *Hamp1* (**d**) mRNA and serum hepcidin (**e**) response to HKBA in tamoxifen-treated i*Hamp1*-KO mice in contrast to tamoxifen-treated i*Hamp1*-Ctrl mice. **f** Lack of hypoferraemic response to HKBA in tamoxifen-treated i*Hamp1*-KO mice. Dot plots show the mean ± SD; p values indicate the results of t tests; in cases where data are spread over orders of magnitude, data are plotted with log scales, geometric means ± geometric SD are shown, and t tests are performed on log-transformed data.

status compared to controls. This problem can be partially alleviated through the use of iron-deficient diets, but iron is still distributed differently in mice lacking hepcidin. For example, although serum iron in germline *Hamp1*-KO mice fed a diet of 4 ppm Fe for 4–6 weeks was comparable to serum iron in wild-type mice fed a diet of 10,000 ppm Fe for 2 weeks, liver iron was significantly higher in the iron-loaded wild-type mice [5].

Here, we developed the i*Hamp*1-KO mouse in which a floxed *Hamp1* gene is inducibly disrupted following the administration of tamoxifen, which activates a $CreER^{T2}$ recombinase. In the absence of tamoxifen, i*Hamp1*-KO mice grow to adulthood with iron indices and hepcidin levels essentially indistinguishable from age-matched Cre-negative controls (i*Hamp1*-Ctrl mice). Upon tamoxifen exposure, hepcidin is efficiently disrupted in all the tissues examined (liver, duodenum, ear, spleen) and in theory in all tissues that are well perfused. The liver is especially well perfused, and so hepcidin may be especially suitable for tamoxifen-induced gene disruption approaches. Three months following hepcidin disruption, mice exhibited high serum iron and ferritin, low spleen non-heme iron, and increased liver non-heme iron that Perl's staining revealed had accumulated in perivenular areas. This pattern is characteristic of more severe hepcidin deficiency models in mice [11, 31], and contrasts with the periportal iron accumulation that occurs in Hfe–/– and TfR2–/– mice [32, 33] and early stages of human hemochromatosis [34].

Next, we followed the effects of tamoxifen injection over shorter periods of time. Mice injected once with tamoxifen showed reduced *Hamp1* mRNA and serum hepcidin peptide 3 days later, although both parameters further declined in mice injected multiple times with tamoxifen. However, the single tamoxifen injection was sufficient to maximally increase serum iron levels and raise Tsat to 100%. Subsequently, we found that only 6 h after a single tamoxifen injection, disruption of the *Hamp1* gene in the liver had occurred to a significant extent. At this time point, effects on liver *Hamp1* mRNA, serum hepcidin and serum iron were already apparent in female mice, becoming highly significant in both female and male mice by 24 h after injection. These data show that gene disruption, decline in gene expression and downstream physiological effect occur rapidly after exposure to tamoxifen.

We then used this model to assess the role of hepcidin in the hypoferraemic response to inflammation. The inflammatory response to each of LPS, Pam3CSK4 and HKBA in the liver was comparable between tamoxifen-induced i*Hamp*1-KO and littermate i*Hamp1*-Ctrl mice, as indicated by *Il6* and *Fga* mRNA upregulation. In controls exposed to pro-inflammatory stimuli, *Hamp1* mRNA and serum hepcidin was increased, while in all but one experiment (males treated with HKBA), significant decreases in serum iron concentrations were observed, as expected. However, in tamoxifen-induced i*Hamp*1-KO mice, liver *Hamp1* mRNA was vastly reduced and not increased by pro-inflammatory stimuli, serum hepcidin peptide was also reduced, and there was no evidence of absolute hypoferraemia. LPS treatment did lead to decreased serum iron in tamoxifen-induced i*Hamp*1-KO mice, but serum iron was still above that of non-LPS-treated i*Hamp1*-Ctrl mice. Although hepcidin peptide alone can induce hypoferraemia [23], and although anti-hepcidin antibody or Spiegelmer can alleviate inflammation-induced hypoferraemia [29, 30, 35], whether hepcidin is absolutely required for hypoferraemia is not clear. Ferroportin transcription can be decreased by inflammation, potentially also contributing to hypoferraemia [36, 37]. Indeed, Deschemin and Vaulont [12] found that germline *Hamp1*-KO mice could still develop hypoferraemia 6 h after LPS injection, potentially due to hepcidin-independent decreases in ferroportin, Dmt1 and Dcytb in the duodenum, while Guida et al. [20] found that inflammation induced by the administration of FSL1 (a TLR2/6 agonist) or Pam3CSK4 to mice decreased the expression of ferroportin in splenic macrophages and induced hypoferraemia 3 h post-injection in a hepcidin-independent fashion. In our experiments, we observed an approximate 10-fold reduction in splenic *Fpn1* mRNA levels in both i*Hamp*1-KO and i*Hamp1*-Ctrl mice. The lack of hypoferraemia in our experiment suggests that in mice in which the baseline iron status is similar to controls (unlike the *Hamp1*-KO mice used by Deschemin and Vaulont [12], or the C326S hepcidin-resistant ferroportin mutant mice used by Guida et al. [20]), transcriptional downregulation of *Fpn1* (and/or *Dmt1*, Dcytb) caused by LPS, Pam3CSK4 or HKBA is insufficient alone to cause hypoferraemia below normal serum iron levels. The relatively lower serum levels in LPS-treated i*Hamp*1-KO mice compared to vehicle-treated i*Hamp*1-KO mice is, however, consistent with a hepcidin-independent contribution to decreases in serum iron during inflammation, which appears to vary depending on the nature of the inflammation-inducing entity. Nevertheless, our experiments show that hepcidin is required for maximal decrease of serum iron to below normal levels by acute inflammation. Hepcidin induction may also be the more important contributor to longer-term inflammatory anaemia because anti-hepcidin treatments can largely rescue serum iron levels and partly restore haemoglobin [21, 29, 30, 35].

In conclusion, we have developed and characterised a new inducible hepcidin-disruption mouse model that illustrates the role of endogenous hepcidin in the rapid control of serum iron under steady-state conditions and in inflammation and infection. The model will allow a detailed investigation of hepcidin in a variety of pathological conditions that involve iron dysregulation.

Acknowledgments

The authors thank Terry Rabbitts and Osama Al-Assar (WIMM, Oxford, UK) for providing *Rosa-CreER^{T2}* mice; Craig Webster (Birmingham Heartlands Hospital, UK) for facilitating the acquisition of serum iron and Tsat data; the staff of the University of Oxford Department of Biomedical Services for animal husbandry; the staff of the Oxford Centre for Histopathology Research (OCHRe) for preparation of histology slides, and Vincenzo Cerundolo, Osama Al-Assar and Philip Hublitz (WIMM, Oxford, UK) for helpful advice and discussions. This work was supported by the Medical Research Council UK (MRC Centenary Award to A.E.A. and M.R.C. Human Immunology Unit core funding to H.D.), a Goodger and Schorstein Scholarship to A.E.A., the British Heart Foundation (Intermediate Science Research Fellowship to S.L.-L.) and by funding from Vifor Pharma to B.D., P.A.R. and S.L.-L. B.D., R.D., D.B. and A.S. were supported by Wellcome Trust Core Award Grant Number 090532/Z/09/Z.

Disclosure Statement

The authors declare no conflicts of interest.

References

1 Ganz T, Nemeth E: Iron homeostasis in host defence and inflammation. Nature Rev Immunol 2015;15:500–510.
2 Payne SM, Finkelstein RA: The critical role of iron in host-bacterial interactions. J Clin Invest 1978;61:1428–1440.
3 Weinberg ED: Iron withholding: a defense against infection and neoplasia. Physiol Rev 1984;64:65–102.
4 Cartwright GE, Lauritsen MA, Jones PJ, Merrill IM, Wintrobe MM: The anemia of infection. I. Hypoferremia, hypercupremia, and alterations in porphyrin metabolism in patients. J Clin Invest 1946;25:65–80.
5 Arezes J, Jung G, Gabayan V, Valore E, Ruchala P, Gulig PA, Ganz T, Nemeth E, Bulut Y: Hepcidin-induced hypoferremia is a critical host defense mechanism against the siderophilic bacterium *Vibrio vulnificus*. Cell Host Microbe 2015;17:47–57.
6 Abboud S, Haile DJ: A novel mammalian iron-regulated protein involved in intracellular iron metabolism. J Biol Chem 2000;275:19906–19912.
7 Donovan A, Brownlie A, Zhou Y, Shepard J, Pratt SJ, Moynihan J, Paw BH, Drejer A, Barut B, Zapata A, Law TC, Brugnara C, Lux SE, Pinkus GS, Pinkus JL, Kingsley PD, Palis J, Fleming MD, Andrews NC, Zon LI: Positional cloning of zebrafish ferroportin1 identifies a conserved vertebrate iron exporter. Nature 2000;403:776–781.
8 McKie AT, Marciani P, Rolfs A, Brennan K, Wehr K, Barrow D, Miret S, Bomford A, Peters TJ, Farzaneh F, Hediger MA, Hentze MW, Simpson RJ: A novel duodenal iron-regulated transporter, IREG1, implicated in the basolateral transfer of iron to the circulation. Mol Cell 2000;5:299–309.
9 Nemeth E, Tuttle MS, Powelson J, Vaughn MB, Donovan A, Ward DM, Ganz T, Kaplan J: Hepcidin regulates cellular iron efflux by binding to ferroportin and inducing its internalization. Science (New York) 2004;306:2090–2093.
10 Zumerle S, Mathieu JR, Delga S, Heinis M, Viatte L, Vaulont S, Peyssonnaux C: Targeted disruption of hepcidin in the liver recapitulates the hemochromatotic phenotype. Blood 2014;123:3646–3650.
11 Lesbordes-Brion JC, Viatte L, Bennoun M, Lou DQ, Ramey G, Houbron C, Hamard G, Kahn A, Vaulont S: Targeted disruption of the hepcidin 1 gene results in severe hemochromatosis. Blood 2006;108:1402–1405.
12 Deschemin JC, Vaulont S: Role of hepcidin in the setting of hypoferremia during acute inflammation. PLoS One 2013;8:e61050.
13 Lakhal-Littleton S, Wolna M, Carr CA, Miller JJ, Christian HC, Ball V, Santos A, Diaz R, Biggs D, Stillion R, Holdship P, Larner F, Tyler DJ, Clarke K, Davies B, Robbins PA: Cardiac ferroportin regulates cellular iron homeostasis and is important for cardiac function. Proc Natl Acad Sci USA 2015;112:3164–3169.
14 Ventura A, Kirsch DG, McLaughlin ME, Tuveson DA, Grimm J, Lintault L, Newman J, Reczek EE, Weissleder R, Jacks T: Restoration of p53 function leads to tumour regression in vivo. Nature 2007;445:661–665.
15 Armitage AE, Eddowes LA, Gileadi U, Cole S, Spottiswoode N, Selvakumar TA, Ho LP, Townsend AR, Drakesmith H: Hepcidin regulation by innate immune and infectious stimuli. Blood 2011;118:4129–4139.
16 Iron Panel of the International Committee for Standardization in Haematology: Revised recommendations for the measurements of the serum iron in human blood. Br J Haematol 1990;75:615–616.
17 Kautz L, Meynard D, Monnier A, Darnaud V, Bouvet R, Wang RH, Deng C, Vaulont S, Mosser J, Coppin H, Roth MP: Iron regulates phosphorylation of smad1/5/8 and gene expression of Bmp6, Smad7, Id1, and Atoh8 in the mouse liver. Blood 2008;112:1503–1509.
18 Yang Q, Jian J, Katz S, Abramson SB, Huang X: 17β-estradiol inhibits iron hormone hepcidin through an estrogen responsive element half-site. Endocrinology 2012;153:3170–3178.
19 Courselaud B, Troadec MB, Fruchon S, Ilyin G, Borot N, Leroyer P, Coppin H, Brissot P, Roth MP, Loreal O: Strain and gender modulate hepatic hepcidin 1 and 2 mRNA expression in mice. Blood Cell Mol Dis 2004;32:283–289.
20 Guida C, Altamura S, Klein FA, Galy B, Boutros M, Ulmer AJ, Hentze MW, Muckenthaler MU: A novel inflammatory pathway mediating rapid hepcidin-independent hypoferremia. Blood 2015;125:2265–2275.
21 Sasu BJ, Cooke KS, Arvedson TL, Plewa C, Ellison AR, Sheng J, Winters A, Juan T, Li H, Begley CG, Molineux G: Anti-hepcidin antibody treatment modulates iron metabolism and is effective in a mouse model of inflammation-induced anemia. Blood 2010;115:3616–3624.
22 Silva B, Faustino P: An overview of molecular basis of iron metabolism regulation and the associated pathologies. Biochim Biophys Acta 2015;1852:1347–1359.
23 Rivera S, Nemeth E, Gabayan V, Lopez MA, Farshidi D, Ganz T: Synthetic hepcidin causes rapid dose-dependent hypoferremia and is concentrated in ferroportin-containing organs. Blood 2005;106:2196–2199.
24 Du X, She E, Gelbart T, Truksa J, Lee P, Xia Y, Khovananth K, Mudd S, Mann N, Moresco EM, Beutler E, Beutler B: The serine protease TMPRSS6 is required to sense iron deficiency. Science (New York) 2008;320:1088–1092.
25 Finberg KE, Heeney MM, Campagna DR, Aydinok Y, Pearson HA, Hartman KR, Mayo MM, Samuel SM, Strouse JJ, Markianos K, Andrews NC, Fleming MD: Mutations in TMPRSS6 cause iron-refractory iron deficiency anemia (IRIDA). Nat Genet 2008;40:569–571.
26 Drakesmith H, Prentice AM: Hepcidin and the iron-infection axis. Science (New York) 2012;338:768–772.
27 Nemeth E, Valore EV, Territo M, Schiller G, Lichtenstein A, Ganz T: Hepcidin, a putative mediator of anemia of inflammation, is a type II acute-phase protein. Blood 2003;101:2461–2463.
28 Nicolas G, Chauvet C, Viatte L, Danan JL, Bigard X, Devaux I, Beaumont C, Kahn A, Vaulont S: The gene encoding the iron regulatory peptide hepcidin is regulated by anemia, hypoxia, and inflammation. J Clin Invest 2002;110:1037–1044.
29 Cooke KS, Hinkle B, Salimi-Moosavi H, Foltz I, King C, Rathanaswami P, Winters A, Steavenson S, Begley CG, Molineux G, Sasu BJ: A fully human anti-hepcidin antibody modulates iron metabolism in both mice and non-human primates. Blood 2013;122:3054–3061.
30 van Eijk LT, John AS, Schwoebel F, Summo L, Vauleon S, Zollner S, Laarakkers CM, Kox M, van der Hoeven JG, Swinkels DW, Riecke K, Pickkers P: Effect of the antihepcidin Spiegelmer lexaptepid on inflammation-induced decrease in serum iron in humans. Blood 2014;124:2643–2646.
31 Meynard D, Kautz L, Darnaud V, Canonne-Hergaux F, Coppin H, Roth MP: Lack of the bone morphogenetic protein BMP6 induces massive iron overload. Nat Genet 2009;41:478–481.
32 Fleming RE, Ahmann JR, Migas MC, Waheed A, Koeffler HP, Kawabata H, Britton RS, Bacon BR, Sly WS: Targeted mutagenesis of the murine transferrin receptor-2 gene produces hemochromatosis. Proc Natl Acad Sci USA 2002;99:10653–10658.
33 Zhou XY, Tomatsu S, Fleming RE, Parkkila S, Waheed A, Jiang J, Fei Y, Brunt EM, Ruddy DA, Prass CE, Schatzman RC, O'Neill R, Britton RS, Bacon BR, Sly WS: HFE gene knockout produces mouse model of hereditary hemochromatosis. Proc Natl Acad Sci USA 1998;95:2492–2497.
34 Iancu TC, Deugnier Y, Halliday JW, Powell LW, Brissot P: Ultrastructural sequences during liver iron overload in genetic hemochromatosis. J Hepatol 1997;27:628–638.
35 Schwoebel F, van Eijk LT, Zboralski D, Sell S, Buchner K, Maasch C, Purschke WG, Humphrey M, Zollner S, Eulberg D, Morich F, Pickkers P, Klussmann S: The effects of the anti-hepcidin Spiegelmer NOX-H94 on inflammation-induced anemia in cynomolgus monkeys. Blood 2013;121:2311–2315.
36 Yang F, Liu XB, Quinones M, Melby PC, Ghio A, Haile DJ: Regulation of reticuloendothelial iron transporter MTP1 (Slc11a3) by inflammation. J Biol Chem 2002;277:39786–39791.
37 Ludwiczek S, Aigner E, Theurl I, Weiss G: Cytokine-mediated regulation of iron transport in human monocytic cells. Blood 2003;101:4148–4154.